Autoinducer 2 Controls Biofilm Formation in *Escherichia coli* through a Novel Motility Quorum-Sensing Regulator (MqsR, B3022)

Andrés F. González Barrios,[1] Rongjun Zuo,[1] Yoshifumi Hashimoto,[2] Li Yang,[2]
William E. Bentley,[2] and Thomas K. Wood[1]*

*Departments of Chemical Engineering and Molecular & Cell Biology, University of Connecticut, 191 Auditorium Rd., Storrs,
Connecticut 06269-3222,[1] and Department of Chemical and Biomolecular Engineering, University of Maryland,
College Park, Center for Biosystems Research, UMBI, College Park, Maryland 20742[2]*

The cross-species bacterial communication signal autoinducer 2 (AI-2), produced by the purified enzymes Pfs (nucleosidase) and LuxS (terminal synthase) from *S*-adenosylhomocysteine, directly increased *Escherichia coli* biofilm mass 30-fold. Continuous-flow cells coupled with confocal microscopy corroborated these results by showing the addition of AI-2 significantly increased both biofilm mass and thickness and reduced the interstitial space between microcolonies. As expected, the addition of AI-2 to cells which lack the ability to transport AI-2 (*lsr* null mutant) failed to stimulate biofilm formation. Since the addition of AI-2 increased cell motility through enhanced transcription of five motility genes, we propose that AI-2 stimulates biofilm formation and alters its architecture by stimulating flagellar motion and motility. It was also found that the uncharacterized protein B3022 regulates this AI-2-mediated motility and biofilm phenotype through the two-component motility regulatory system QseBC. Deletion of *b3022* abolished motility, which was restored by expressing *b3022* in *trans*. Deletion of *b3022* also decreased biofilm formation significantly, relative to the wild-type strain in three media (46 to 74%) in 96-well plates, as well as decreased biomass (8-fold) and substratum coverage (19-fold) in continuous-flow cells with minimal medium (growth rate not altered and biofilm restored by expressing *b3022* in *trans*). Deleting *b3022* changed the wild-type biofilm architecture from a thick (54-μm) complex structure to one that contained only a few microcolonies. B3022 positively regulates expression of *qseBC*, *flhD*, *fliA*, and *motA*, since deleting *b3022* decreased their transcription by 61-, 25-, 2.4-, and 18-fold, respectively. Transcriptome analysis also revealed that B3022 induces *crl* (26-fold) and *flhCD* (8- to 27-fold). Adding AI-2 (6.4 μM) increased biofilm formation of wild-type K-12 MG1655 but not that of the isogenic *b3022*, *qseBC*, *fliA*, and *motA* mutants. Adding AI-2 also increased *motA* transcription for the wild-type strain but did not stimulate *motA* transcription for the *b3022* and *qseB* mutants. Together, these results indicate AI-2 induces biofilm formation in *E. coli* through B3022, which then regulates QseBC and motility; hence, *b3022* has been renamed the motility quorum-sensing regulator gene (the *mqsR* gene).

There is an explosive amount of research on biofilms with the ultimate aim of their control (24); however, little is known about the regulation of this complex process of cell attachment leading to exquisite architecture (11). Since 65% of human bacterial infections involve biofilms (31), understanding the genetic basis of biofilm formation to find effective ways to prevent biofilms is important for combating disease and for engineering applications. To this end, we have studied the whole bacterial genome with DNA microarrays by two complementary approaches: studying biofilm gene expression relative to planktonic cells (34, 35) and studying plant-derived biofilm inhibitors that do not alter the bacterial growth rate, such as ursolic acid (38) and (5*Z*)-4-bromo-5-(bromomethylene)-3-butyl-2(5*H*)-furanone (furanone) of the alga *Delisea pulchra* (36, 37). We found that furanone inhibits *Escherichia coli* biofilm formation and that 80% of the genes that were repressed by furanone were induced by cross-species quorum-sensing signal autoinducer 2 (AI-2) (36); hence, AI-2 should stimulate biofilm formation.

Bacteria use quorum sensing to regulate some forms of gene expression by sensing their population density via small signaling compounds that are secreted into the environment (3). AI-2 is produced by LuxS, is a species-nonspecific signal used by both gram-negative and gram-positive bacteria (47), and has been found in at least 55 strains (4). Three groups have used DNA microarrays to show AI-2 controls 166 to 404 genes, including those for chemotaxis, flagellar synthesis, motility, and virulence factors in *E. coli* (15, 36, 44). However, the species-nonspecific signal AI-2 has not been shown directly to control biofilms.

Quorum sensing has been linked to biofilms previously, since a species-specific signal, *N*-(3-oxododecanoyl)-L-homoserine lactone, has been shown to influence biofilm formation in *Pseudomonas aeruginosa* (14). In addition, quorum sensing controls biofilm formation by controlling exopolysaccharide synthesis in *Vibrio cholerae* (which has homoserine lactone and AI-2 signals) (19), by controlling cell aggregation in *Serratia liquefaciens* (which has a homoserine lactone signal) (24), and by controlling genetic competence in *Streptococcus mutans* (which has a peptide signal) (25). AI-2 has been found to influence biofilm formation in a mixed-species biofilm between *Streptococcus gordonii* and *Porphyromonas gingivalis* (26) and has been shown to impact slightly the architecture of *Klebsiella pneu-*

TABLE 1. *E. coli* strains and plasmids used[a]

Strain or plasmid	Genotype	Source
Strains		
Vibrio harveyi BB170	BB120 *luxN*::Tn5 (AI-1 sensor⁻, AI-2 sensor⁺)	46
E. coli K-12	Wild type	ATCC 25404
E. coli DH5α	*luxS supE44 ΔlacU169* (φ80d*lacZ*ΔM15) *hsdR17 recA1 endA1 gyrA96 thi-1 relA1*	36
E. coli K-12 BW25113	*lacI*q *rrn*$_{B_{T14}}$ Δ*lacZ*$_{WJ16}$ *hsdR514* Δ*araBAD*$_{AH33}$ Δ*rhaBAD*$_{LD78}$	13
E. coli K-12 BW25113 Δ*luxS*	K12 Δ*luxS*::Km^r	1
E. coli JM109	*recA1 supE44 endA1 hsdR17 gyrA96 relA1 thi* Δ(*lac-proAB*) F′ [*traD36 proAB*⁺ *lacI*q *lacZ*ΔM15]	54
E. coli K-12 MG1655	F⁻ λ⁻ *ilvG rfb-50 rph-1*	5
E. coli K-12 MG1655 Δ*motA*	Δ*motA*::Tn5Kan-2	23
E. coli K-12 MG1655 Δ*qseB*	Δ*qseB*::Tn5Kan-2	23
E. coli K-12 MG1655 Δ*lsrK*	Δ*lsrK*::Tn5Kan-2	23
E. coli K-12 MG1655 Δ*fliA*	Δ*fliA*::Tn5Kan-2	23
E. coli K-12 MG1655 Δ*mqsR*	Δ*b3022*::Tn5Kan-2	23
E. coli W3110	Wild type	21
Plasmids		
R1*drd19*	Amp^r Km^r Cm^r Sm^r; IncFII *finO*	18
pTrcHis-pfs	Amp^r; pTrcHisC (Invitrogen) with *pfs* from *E. coli* strain W3110	21
pTrcHis-luxS	Amp^r; pTrcHisC (Invitrogen) with *luxS* from *E. coli* strain W3110	21
pCM18	Em^r; pTRKL2-P$_{CP25}$-RBSII-*gfp*mut3*-T$_0$-T$_1$ (GFP plasmid for visualizing biofilm)	20
pCA24N	Cm^r; *lacI*q	1
pCA24N *luxS*⁺	Cm^r; *lacI*q; P$_{T5-lac}$ *luxS*	1
pVLT31 *mqsR*⁺	pVLT31 *plac*::*mqsR*⁺	This study
pVS159	Amp^r; *qseB*::*lacZ* in pRS551	45
pVS176	Amp^r; *motA*::*lacZ* in pRS551	45
pVS175	Amp^r; *fliC*::*lacZ* in pRS551	45
pVS183	Amp^r; *fliAehK12*::*lacZ* in pRS551	45
pVS182	Amp^r; *flhD*::*lacZ* in pRS551	45

[a] Amp^r, Km^r, Cm^r, Sm^r, Em^r, Rif^r, and Tc^r, ampicillin, kanamycin, chloramphenicol, streptomycin, erythromycin, rifampin, and tetracycline resistance, respectively.

moniae (although no effect of AI-2 on biofilm formation was found using a *luxS* mutant for intestinal colonization and colonization on polystyrene) (2) and to affect attachment in *Helicobacter pylori* (a *luxS* homolog has been found that negatively regulates biofilm formation) (10). For these few AI-2 results with biofilms, mutants or conditioned media were used rather than the signal itself and the role of AI-2 was not clear; indeed, a recent report indicates that LuxS has no effect on biofilm formation of *Haemophilus influenzae* (12). Here, we show conclusively that synthesized AI-2 directly stimulates biofilm formation in *E. coli*, that it controls biofilm architecture, that it controls this phenotype by stimulating bacterial motility, and that it does this through the uncharacterized protein MqsR (B3022).

Although the *E. coli* locus *mqsR* (b3022) was found to be induced eightfold in biofilms (35), there is little information about the function of MqsR. MqsR appears to be a conserved regulator protein (98 amino acids), since it has >50% homology with hypothetical proteins from *Yersinia pseudotuberculosis*, *Yersinia pestis*, *Cupriavidus oxalaticus*, *Bordetella bronchiseptica*, *Pseudomonas fluorescens*, and *Bordetella pertussis* (8, 27, 29, 43, 48). As part of the 300-gene, quorum-sensing regulon in *E. coli* (15, 36, 44), *qseBC* (b3025 and b3026) are organized in an operon in the *E. coli* chromosome with QseB playing a role as a response regulator and QseC playing a role as the sensor kinase (45). Flagellum expression is temporally regulated, and the operons are divided into early, middle, and late genes. QseBC regulates transcription of the master regulon *flhDC* and therefore expression of the middle operon (e.g., *fliA* encoding sigma factor σ²⁸) and late operon (e.g., *fliC* encoding flagellin and *motA*

encoding the proton exchange conductor for flagellum movement) (9). Here, we determined that MqsR controls biofilm formation in *E. coli* by positively regulating *qseBC*; hence, MqsR is the mediator between AI-2 and motility.

MATERIALS AND METHODS

Bacterial strains, growth media, and toxicity testing. The strains and plasmids of this study are listed in Table 1. Luria-Bertani medium (LB) (41) was used to preculture all the *E. coli* cells. LB, minimal M9 medium with 0.4% (wt/vol) Casamino Acids and 0.8-g/liter sodium citrate (M9C citrate) (40), LB supplemented with 0.2% (wt/vol) glucose (LB glu), and M9 supplemented with 0.4% (wt/vol) glucose and 0.4% (wt/vol) Casamino Acids (M9C glu) were used for the 96-well biofilm experiments. For the flow cell experiments, M9C glu medium was

TABLE 2. Effect of AI-2 on the biofilm formation of *E. coli* ATCC 25404, DH5α, and MG1655 in LB medium and 96-well plates[a]

E. coli strain	AI-2 (μM)	Total biofilm (OD$_{540}$)	Fold change
ATCC 25404	0	0.05 ± 0.02	1
	0.2	0.4	6.8 ± 0.9
	3.2	1.0 ± 0.2	17.4 ± 0.7
	11	1.5 ± 0.4	26 ± 2
DH5α	0	0.01 ± 0.05	1
	0.2	0.05 ± 0.02	3.9 ± 0.6
	3.2	0.3 ± 0.3	25.0 ± 0.9
	11	0.4 ± 0.2	28.9 ± 0.3
MG1655	0	0.41 ± 0.02	1
	0.2	0.5 ± 0.1	1.2 ± 0.5
	3.2	1.0 ± 0.1	2.5 ± 0.3
	11	1.6 ± 0.5	4 ± 2

[a] Biomass measured at 24 h. Each experiment was performed twice, and one standard deviation is shown.
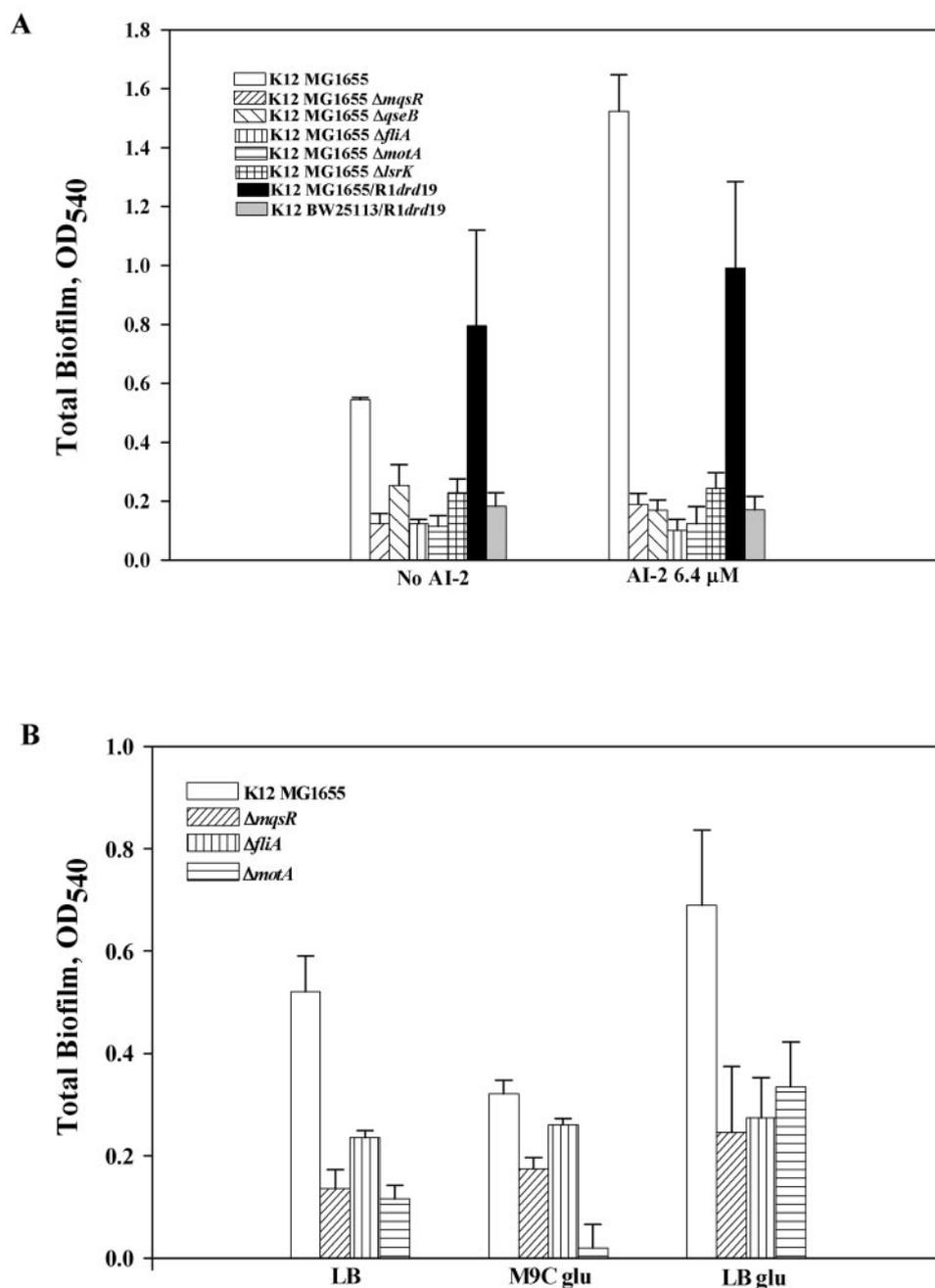
FIG. 1. Effects of *mqsR*, *qseB*, *fliA*, *motA*, *lsrK*, and the R1*drd*19 conjugation plasmid on biofilm formation upon the addition of 6.4 μM AI-2 in LB medium (A) and effects of *mqsR*, *fliA*, and *motA* on the biofilm formation of MG1655 in LB, M9C glu, and LB glu media (B). Homocysteine and adenine (each, 6.4 μM) were added as the negative control when AI-2 effect was evaluated (A). Biomass was measured after 24 h. Each experiment was performed in duplicate, and 1 standard deviation is shown.

used for MG1655 and MG1655 Δ*mqsR*, and LB was used for ATCC 25404. For purification of Pfs and LuxS, *E. coli* DH5α carrying pTrcHis-pfs or pTrcHis-luxS from *E. coli* W3110 (21) was cultured in SOB medium (20 g of tryptone/liter, 5 g of yeast extract/liter, 0.5 g of sodium chloride/liter, 2.5 mM potassium chloride, and 10 mM magnesium chloride) (41).

Construction of the complementation plasmid pVLT31 *mqsR*⁺. To show that the *mqsR* gene is responsible for the altered motility phenotype, a complementation plasmid was constructed using the low-copy-number plasmid pVLT31 (16). The whole coding sequence of *mqsR* was amplified using the primer pair pA (front primer, 5′-GGTTATAACTGAATTCACAGGGAGGCGGGG-3′) and pB (rear primer, 5′-GCCAGAAACCATTTCTAGATGGTGGCAAACCGG-3′). The PCR

product was digested with EcoR I and XbaI and cloned into the multiple cloning site of pVLT31 that was digested with the same two enzymes to create the complementation plasmid pVLT31 *mqsR*⁺. This recombinant plasmid was confirmed through DNA sequencing upstream of the *ptac* promoter using primer pC (5′-GAGCGG ATAACAATTTCACACAGG-3′). Since pVLT31 carries *lacI*�q, expression of the *mqsR*⁺ gene requires isopropyl-β-D-thiogalactopyranoside (IPTG; Sigma, St. Louis, Mo.), which was added at 0.4 mM for complementing motility and at 0.2 mM for complementing biofilm formation of the *mqsR* mutant.

Synthesis of AI-2. At an optical density at 600 nm (OD₆₀₀) of 0.4 to 0.6, 1 mM IPTG was added to induce expression of His-Pfs or His-LuxS. After 4 h of induction, cells were collected by centrifugation at 14,000 × *g* for 20 min at 4°C.

The cells were stored at −80°C and lysed using BugBuster solution (Novagen) (300 μl and 2.5 ml culture pellets for His-Pfs or 1.5 ml and 50 ml culture pellets for His-LuxS) for 20 min at room temperature. Soluble cell extracts were collected by centrifugation at $14,000 \times g$ for 20 min at 4°C, mixed with Co^{2+} affinity resin (BD TALON; BD Biosciences), and washed with equilibration-wash buffer (50 mM sodium phosphate, 0.3 M sodium chloride [pH 7.0]). Twenty microliters and 600 μl of Co^{2+} resin suspension were mixed with the soluble cell extracts from the 2.5-ml and 50-ml cultures. His-Pfs or His-LuxS was bound to the Co^{2+} resin, and the Co^{2+} resin was washed to remove nonspecifically bound proteins as described in the manufacturer's protocol. The bound proteins were eluted with 300 μl of elution buffer (125 mM imidazole in equilibration-wash buffer) containing 100 μM zinc chloride, 10 mM β-mercaptoethanol, and 1 mM phenylmethylsulfonyl fluoride. His-tagged protein purification was performed at 0°C, Co^{2+} resin was removed by centrifugation, and the supernatant was extracted twice with chloroform. Image analysis of sodium dodecyl sulfate-polyacrylamide gel electrophoresis gels indicated Pfs (28,899 Da) and LuxS (23,962 Da) were highly purified (>99%; data not shown), and no other bands were seen. In addition, no other immunoreactive bands were detected by using anti-His immunoblots.

The purified Pfs and LuxS enzymes were used to synthesize AI-2 from 1 mM S-adenosylhomocysteine in 50 mM Tris-HCl, pH 7.8 (41), containing 100 μM zinc chloride and 1 mM phenylmethylsulfonyl fluoride. In vitro AI-2 synthesis reactions were carried out at 37°C overnight. Concentrations of His-Pfs and His-LuxS in the reaction mixtures were 8 μM and 69 μM, respectively. High-performance liquid chromatography showed complete conversion of SAH by Pfs, as well as the complete conversion of S-ribosylhomocysteine by LuxS in the AI-2 samples.

Autoinducer activity assay. Activity of the synthesized AI-2 was assayed as described previously (46). Briefly, the reporter strain *Vibrio harveyi* BB170 was grown in autoinducer bioassay medium (0.3 M NaCl, 0.05 M $MgSO_4$, 0.2% Casamino Acids, 10 μM KH_2PO_4, 1 μM L-arginine, 20% glycerol, 0.01 μg/ml riboflavin, and 1 μg/ml thiamine) overnight and diluted 1:5,000 into the fresh AB medium, and then AI-2 was added at 0.2, 0.4, 0.8, or 1.6 μM. The time course of bioluminescence was measured with a 20/20 luminometer (Turner Design, Sunnyvale, CA) and reported as relative light units. The cell density of the *V. harveyi* reporter strain was measured by spreading the cells on Luria marine medium (20 g/liter NaCl, 10 g/liter Bacto tryptone, and 5 g/liter yeast extract) plates and counting the CFU after 24 h. Each experiment was conducted in duplicate. The optimum concentration of AI-2 for bioluminescence (0.8 μM) was used as the basis for evaluating the effect of AI-2 on *E. coli* biofilm formation (0.8, 1.6, 3.2, and 6.4 μM).

Crystal violet biofilm assay. This assay was adapted from those reported previously (32). *E. coli* was grown in polystyrene 96-well plates at 37°C for 2 days without shaking in LB medium, M9C glu, LB glu medium, or M9C citrate supplemented with AI-2. Each data point was averaged from four replicate wells, and the standard deviations were calculated. Plates were processed after 24 h. The experiments were conducted twice using two independent cultures with each culture evaluated in four wells (total of eight wells). Negative controls were wells containing 11 μM (each) adenine and homocysteine.

Flow cell biofilm experiments and image analysis. LB medium was supplemented with 200-μg/ml erythromycin to maintain pCM18 (20) (Table 1), which contains the constitutive green fluorescent protein (GFP) vector and which allows visualization of the biofilm. The biofilm was formed at 37°C in a continuous flow cell that consists of a standard glass microscope slide on one side and a plastic coverslip on the other side with dimensions of 47.5 mm by 12.7 mm with a 1.6-mm gap between the surfaces (BST model FC81; Biosurface Technologies Corp., Bozeman, MT). Overnight cultures in LB medium supplemented with 120- to 200-μg/ml erythromycin (to retain the GFP plasmid pCM18) were centrifuged and resuspended in LB medium with erythromycin. This diluted culture (OD$_{600}$, 0.05) was used to inoculate the flow cell for 2 h at a flow rate of 10 ml/h before fresh LB or M9C glu medium flow with erythromycin was started at the same flow rate; the initial inoculum was 1.5×10^8 cells/ml. To determine the impact of AI-2, 6.4 μM AI-2 was added upon inoculation and in the continuous feed or homocysteine and adenine were added (each, 6.4 μM) as the negative control. Biofilm development in the flow cell was monitored with a TCS SP2 scanning confocal laser microscope (Leica Microsystems, Heidelberg, Germany) with a 40× objective at 16 and 24 h.

Color confocal flow cell images were converted to grayscale using Image Converter (Neomesh Microsystems, Wainuiomata, Wellington, New Zealand). Biomass, substratum coverage, surface roughness, and mean thickness were determined with COMSTAT image-processing software (22) written as a script in Matlab 5.1 (The MathWorks) and equipped with the Image Processing Toolbox. Thresholding was fixed for all image stacks. At each time point, nine

TABLE 3. Biofilm COMSTAT flow cell measurements for the addition of 6.4 μM AI-2 to ATCC 25404 and for the *luxS* (*E. coli* DH5α) and *mqsR* mutations

Strain and time after inoculation (h)	Condition(s) or parameter	Biomass ($\mu m^3/\mu m^2$)	Substratum coverage (%)	Mean thickness (μm)	Roughness coefficient
ATCC 25404 (16)	No AI-2 6.4 μM AI-2 Ratio	9 ± 3 48 ± 17 5	41 ± 4 55 ± 16 1.3	12 ± 2 86 ± 13 7	0.9 ± 0.1 0.3 ± 0.1 −3.5
ATCC 25404 (24)	No AI-2 6.4 μM AI-2 Ratio	15 ± 4 68 ± 9 4.5	57 ± 7 71 ± 7 1.2	25 ± 7 94 ± 14 3.7	0.6 ± 0.2 0.20 ± 0.08 −2.9
DH5α (24)	No AI-2	8 ± 3	41 ± 11	10 ± 4	1.0 ± 0.2
MG1655 (24)	No AI-2	25 ± 8	34 ± 14	44 ± 6	0.2 ± 0.1
MG1655 ΔmqsR (24)	No AI-2	5.6 ± 1.6	5 ± 2	27 ± 22	1.5 ± 0.4
MG1655 (48)	No AI-2	35 ± 30	45 ± 10	54 ± 30	0.8 ± 0.6
MG1655 ΔmqsR (48)	No AI-2	4.4 ± 7	2.4 ± 1.3	13 ± 5	1.7 ± 0.5

different positions were chosen for microscope analysis, and 225 images were processed for each time point. Values are means of data from the different positions at the same time point, and standard deviations were calculated based on these mean values for each position. Simulated three-dimensional images were obtained by using IMARIS (BITplane, Zurich, Switzerland). Twenty-five pictures were processed for each three-dimensional image.

Motility assay. LB overnight cultures were used to assay motility in plates containing 1% tryptone, 0.25% NaCl, and 0.3% agar (45). The motility halos were measured at 8 h for ATCC 25404, MG1655, and MG1655 ΔmqsR/pVLT31 mqsR$^+$ and at 16 h for DH5α, JM109, and BW25113. Between 3 and 25 plates were used to evaluate motility in each strain. Motility agar plates containing AI-2 (0.8 or 3.2 μM) were used to test the impact of AI-2 on motility, and homocysteine and adenine (each, 0.8 or 3.2 μM) were added to the agar as a negative control. Each experiment was performed in duplicate.

Transcription reporter assays. To determine the effect of AI-2 on the expression of the motility genes, ATCC 25404 cultures with the *lacZ* fusion transcriptional reporters *qseB::lacZ*, *flhD::lacZ*, *fliA::lacZ*, *fliC::lacZ*, and *motA::lacZ* (45) were cultured overnight in LB ampicillin (100 μg/ml), diluted 1:100 in LB medium, and then grown to stationary phase to an OD$_{600}$ of 3, since internalization of AI-2 takes place primarily in stationary phase (53). Once cells reached stationary phase, AI-2 was added at 6.4 μM for 2 h (adenine and homocysteine were added, each at a concentration of 6.4 μM, as a negative control). β-Galactosidase activity was evaluated as described previously (51). All activities were calculated based on a protein concentration of 0.24 mg of protein/ml/OD$_{600}$ unit (17).

To determine the effect of *mqsR* and *qseB* on the expression of the motility genes, MG1655 and MG1655 ΔmqsR were cultured overnight in LB ampicillin (100 μg/ml), diluted 1:100 in LB medium, and grown to exponential phase to an OD$_{600}$ of 1. When the effect of AI-2 on *qseB* expression in MG1655 and MG1655 ΔmqsR was tested, cells were cultured overnight in LB ampicillin (100 μg/ml), diluted 1:100 in M9C glu medium, different concentrations of AI-2 (0, 3.2, and 6.4 μM) were added, and the cells were grown to exponential phase (OD$_{600}$ of 1). Homocysteine and adenine (each, 6.4 μM) were added to cultures as a negative control. The same procedure was followed for testing *qseB* expression in MG1655 ΔmqsR complemented with pVLT31 mqsR$^+$, but instead of AI-2, IPTG was added at different concentrations (0, 0.1, 0.2, 0.4, and 1 mM).

Microarray analysis. The strains were cultured in LB medium overnight (with kanamycin added to MG1655 ΔmqsR), diluted 1:100 in LB medium, and grown to exponential phase (OD$_{600}$, 1); total RNA was isolated as described previously (35). The Affymetrix *E. coli* GeneChip antisense genome array (catalogue no. 900381), which contains probe sets for all 4,290 open reading frames, rRNA, tRNA, and 1,350 intergenic regions, was used to study the effect of the *mqsR* deletion on the gene expression profile of *E. coli*. Briefly, the total RNA samples were first converted into cDNA through a reverse transcription reaction with poly(A) RNA controls spiked into the same reaction mixture to monitor the entire target labeling process. The

A   ATCC 25404, No AI-2

B   ATCC 25404, 6.4 μM AI-2

C   MG1655
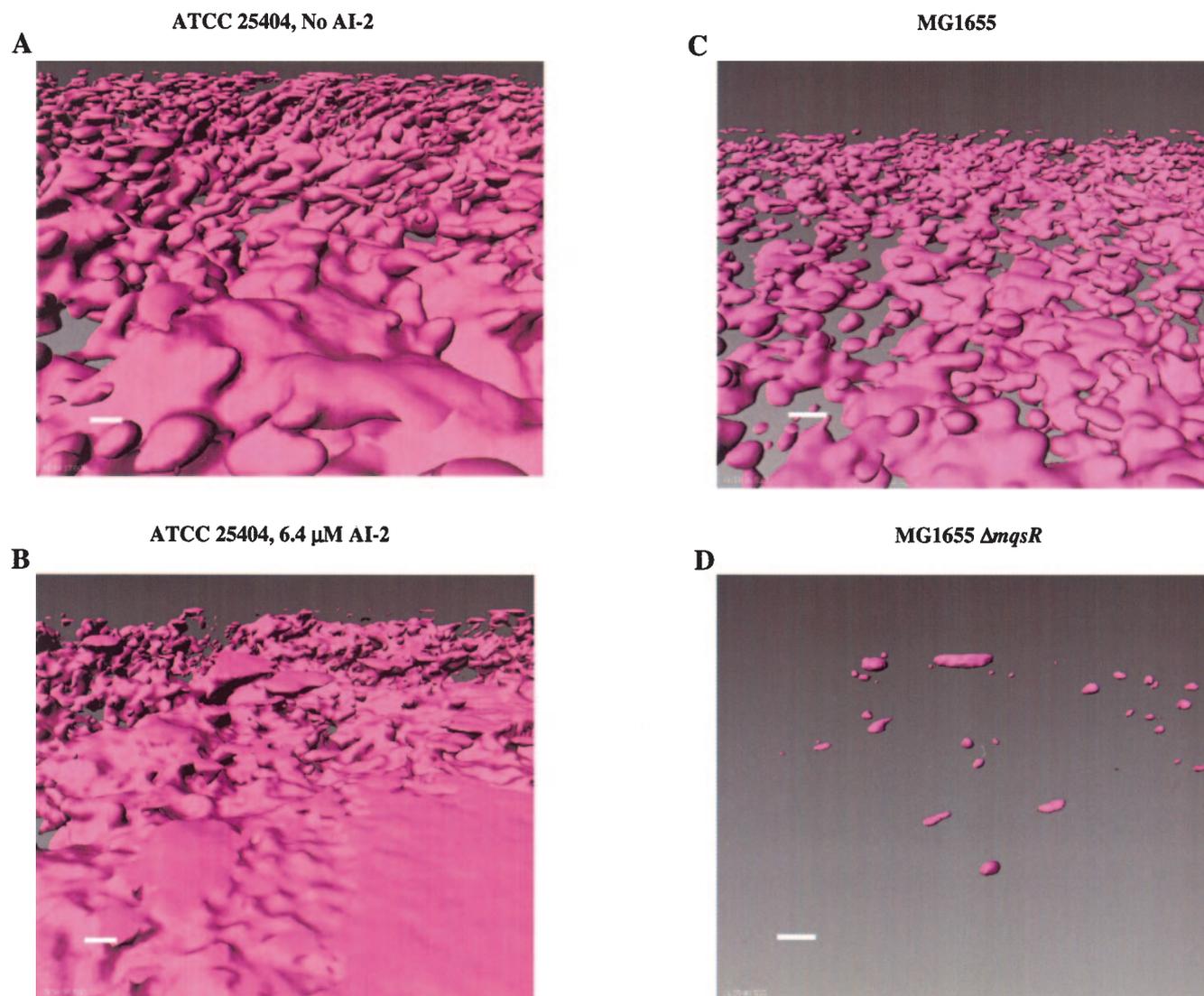
D   MG1655 Δ*mqsR*

FIG. 2. Effects of AI-2 and MqsR on biofilm formation in flow cells at 24 h. ATCC 25404 with no AI-2 (A); ATCC 25404 with 6.4 μM AI-2 (B); MG1655 (C); MG1655 Δ*mqsR* (D). Scale bar, 5 μm.

cDNA was then digested with DNase I (Amersham Biosciences) to produce 50- to 200-bp fragments, which were checked by running the fragmented cDNA on a 2% agarose gel. The fragmented cDNA was labeled at the 3′ termini by the Enzo BioArray Terminal Labeling kit with Biotin-ddUTP (catalogue no. 900181; Affymetrix). The biotin-labeled target was hybridized to the Affymetrix GeneChip *E. coli* antisense array at 45°C for 16 h at 60 rpm using the Hybridization Oven 640 (Affymetrix), and then a three-step fluorescent staining was conducted using the Fluidics Station 450 (Affymetrix) during the washing and staining procedure. This includes binding of streptavidin to the biotin-labeled cDNA in the first staining solution, binding of biotin-conjugated streptavidin antibody to the streptavidin in the second staining solution, and binding of phycoerythrin-conjugated streptavidin to the biotin-labeled antibody in the third staining solution. The microarray was scanned at 570 nm to get an image file with the GeneChip Scanner 3000 (Affymetrix). Using GeneChip Operating Software, individual strain reports for both the wild-type strain and mutant cDNA samples were obtained, as well as reports comparing the *mqsR* mutant to wild-type *E. coli*. Total cell intensity was scaled automatically in the software to an average value of 500. Since the standard deviation for the expression ratio for all the genes was 2.7, genes with a ≥4-fold change in intensity between the two chips and a *P* value of <0.05 were considered differentially expressed.

RESULTS

AI-2 stimulates *E. coli* biofilm formation in 96-well plates. We suspected AI-2 was involved directly in biofilm formation, since our microarray data indicated that AI-2 controls motility-related genes (e.g., *cheABRWYZ*, *flgABCDEFGHI JKLMN*, *fliACDFHKLMNOPQ*, and *motAB*) (36) and since the plant-derived furanone inhibits biofilms and represses the same AI-2-controlled genes (36). To investigate this hypothesis, we synthesized AI-2 (there is no commercial source) using two *E. coli* enzymes and found it was active via a 2,400-fold increase in bioluminescence in the *V. harveyi* BB170 reporter (0.8 μM AI-2). Then, this active AI-2 (0.2 to 11 μM) was evaluated for its effect on the biofilm formation of three *E. coli* wild-type strains (ATCC 25404, MG1655, and BW25113), the LuxS-deficient strains *E. coli* BW25113 Δ*luxS* and *E. coli* DH5α, and the well-known laboratory
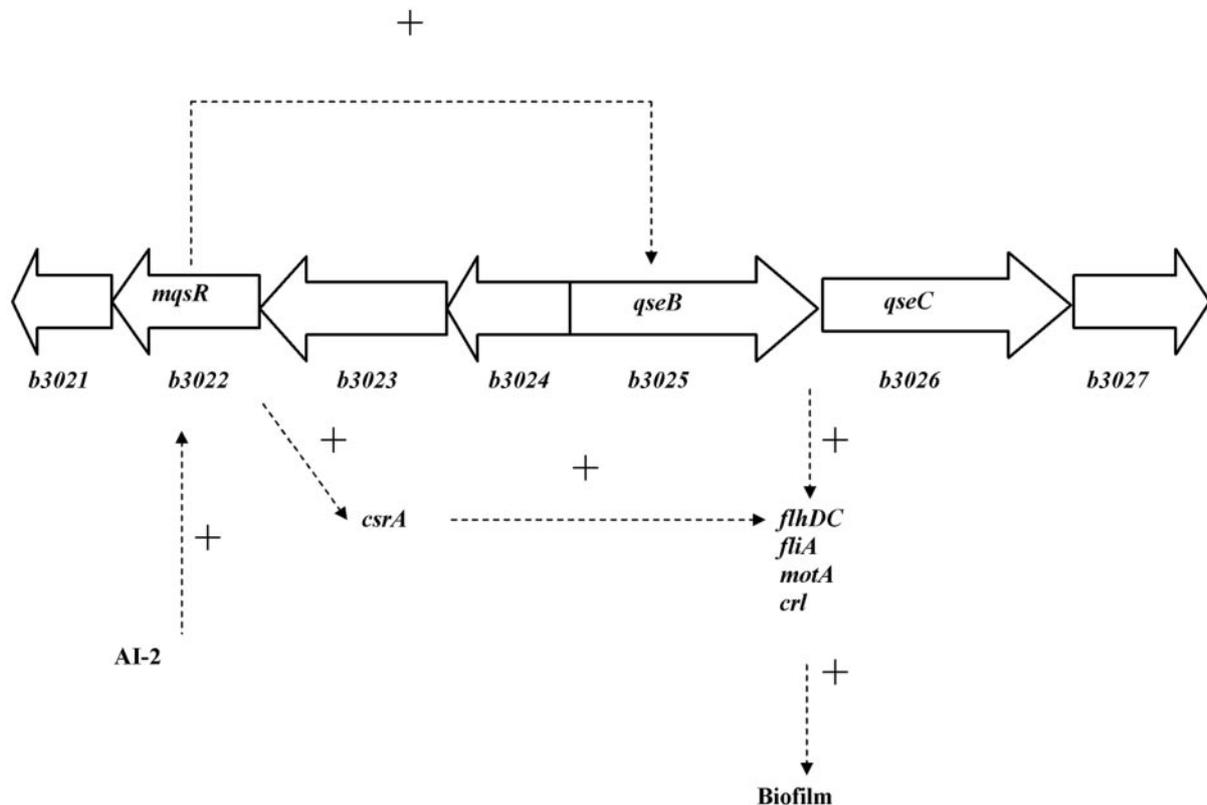
FIG. 3. Model for quorum-sensing regulation of biofilms. AI-2 increases expression of MqsR; which increases expression of QseBC and CsrA; which increases expression of FlhDC, FliA, MotA, and Crl; which results in biofilm stimulation. Plus signs indicate positive regulation (shown by dashed lines).

strain *E. coli* JM109. Biofilm formation was stimulated significantly by 11 μM AI-2 in LB medium at 24 h for ATCC 25404 (26 ± 2 fold), DH5α (29 ± 0.3 fold), and MG1655 (4 ± 2 fold) (Table 2). Biofilm formation was also stimulated in JM109 and BW25113 (2 ± 1 fold at 3.2 μM) and in the *luxS* mutant of BW25113 (1.7 ± 0.3 fold at 1.25 μM). These results with rich media were corroborated with M9C citrate, where 3.2 μM AI-2 stimulated biofilm formation after 24 h for DH5α (2.2 ± 1 fold) and JM109 (1.7 ± 0.4 fold).

Note that in the absence of AI-2, BW25113 ΔluxS made 50% less biofilm than the isogenic wild-type strain, which indicates again that AI-2 stimulates biofilm formation in *E. coli*, since LuxS forms AI-2. Biofilm could be restored by adding complementing *luxS* in *trans* using plasmid pCA24N *luxS*+ (46% of the wild-type biofilm was formed at 0 mM IPTG and 110% of the wild-type biofilm was formed at 0.25 mM IPTG in LB medium).

To confirm that AI-2 was the cause of the increase in biofilm formation, we measured biofilm stimulation with the isogenic MG1655 *lsrK* mutant because this mutation dramatically impairs the AI-2 uptake compared with other mutations in the *lsr* system (49, 52). As expected, AI-2 was not able to induce biofilm formation of the *lsrK* mutant at 6.4 μM (Fig. 1A); hence, AI-2 induces biofilm formation through the LsrK transport pathway (49).

E. coli DH5α, which is deficient in AI-2 synthesis (36) and which was found here to be completely nonmotile, was also studied using the continuous flow cell to see the effect of the *luxS* mutation on biofilm formation (Table 3) and architecture (image not shown). Although we recognize that this strain is not isogenic with ATCC 25404, we thought it might be informative to see if it responded to AI-2 and to look at its architecture. Compared with ATCC 25404 without AI-2, DH5α displayed less biomass (15 ± 4 μm³/μm² versus 8 ± 3 μm³/μm²), less substratum coverage (57% ± 7% versus 41% ± 11%), and less thickness (25 ± 7 μm versus 10 ± 4 μm).

We also tested the effect of AI-2 (6.4 μM) on biofilm formation when strains harbored the derepressed conjugation plasmid R1drd19, which enhances biofilm formation (Fig. 1A) (18). Biofilm formation was not significantly induced with either MG1655 or BW25113 when R1drd19 was present.

AI-2 promotes *E. coli* biofilm formation in a continuous flow cell. To further investigate the effect of AI-2 on biofilm architecture, as well as to corroborate the 96-well plate crystal violet results, a continuous flow cell with LB medium was used to study the biofilm of ATCC 25404 (harboring the GFP plasmid pCM18). In the absence of AI-2, ATCC 25404 developed regular microcolonies covering 41 and 57% of the surface at 16 and 24 h, respectively (Table 3; Fig. 2A); previously similar structures were seen for *E. coli* SAR18 and MG1655 (33). The addition of 6.4 μM AI-2 also led to the formation of typical microcolonies (Fig. 2B), but the amount of attached cells was greater, since the biomass and thickness increased 5-fold ± 3-fold and 7-fold ± 2-fold at 16 h and 5-fold ± 1-fold and 4-fold ± 1-fold at 24 h, respectively. The roughness coefficient
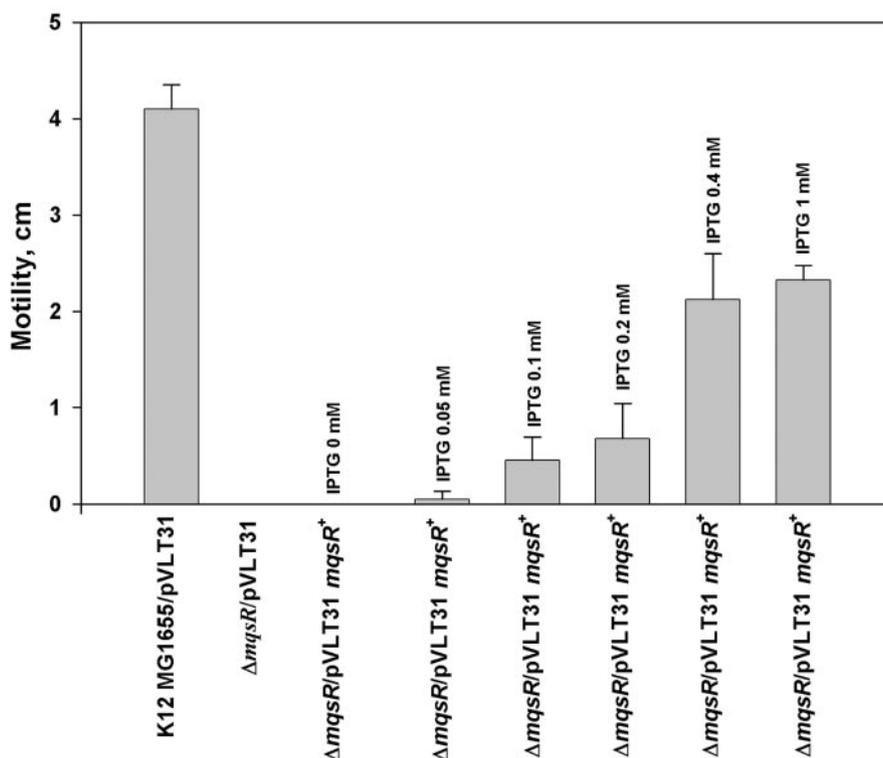
FIG. 4. Effect of deleting *mqsR* on the motility of MG1655 and complementation of motility of using MqsR provided in *trans*. The motility diameter was measured at 8 h. For the complementation experiments, IPTG was added to all cultures; no effect from the addition of IPTG was found with the negative controls (MG1655 Δ*mqsR*/pVLT31, MG1655/pVLT31, and MG1655/pVLT31 *mqsR*⁺). Each experiment was done in duplicate, and 1 standard deviation is shown.

(3-fold ± 1-fold decrease) (Table 3 and Fig. 2) indicated that there was less heterogeneity when AI-2 is added, since the biofilm had fewer interstitial spaces at both times analyzed.

AI-2 increases motility in *E. coli* through QseB. To determine how AI-2 stimulates biofilm formation in *E. coli*, we investigated whether AI-2 addition affected the motility of five strains, since our microarrays (36) indicated that these genes were induced by AI-2 (determined by using a *luxS* mutant). The motility of both ATCC 25404 and MG1655 increased about 30% upon the addition of 0.8 μM AI-2. It was necessary to increase the AI-2 dose to 3.2 μM to see an effect with DH5α and BW25113 (80% and 43% increases in motility, respectively). JM109 did not respond significantly to AI-2 addition at 3.2 μM.

To discern the genetic basis of this increase in motility upon AI-2 addition, we probed the ability of AI-2 to induce the promoters of motility genes *qseB*, *flhD*, *fliA*, *fliC*, and *motA*. Upon addition of 6.4 μM AI-2, the quorum-sensing flagellum regulon *qseB* (45) was induced 8-fold ± 3-fold. These results corroborated the ones reported by Sperandio et al. (45), who previously found that *qseB* was induced 17-fold compared with the *luxS* mutant through DNA microarray studies with *E. coli* O157:H7 and its isogenic *luxS* mutant. The induction of *qseB* here led to a 4.0-fold ± 0.1-fold increase in the transcription of *flhD* (master controller of the flagellum regulon), a 2.6-fold ± 0.3-fold increase in *fliA* (sigma factor σ²⁸), a 3.6-fold ± 0.8-fold increase in *fliC* (flagellin), and a 6-fold ± 0.3-fold increase in *motA* (proton conductor for flagellum movement).

Based on this increase in motility through QseB upon AI-2 addition, we hypothesized that AI-2 induces biofilm formation by inducing motility and that this increase in motility leads to increased attachment. To test our hypothesis, we measured biofilm formation upon the addition of AI-2 to two motility-deficient strains. We added AI-2 to the paralyzed isogenic MG1655 Δ*motA* mutant (9) (we confirmed that this strain is nonmotile), which has reduced biofilm formation (32), and to the isogenic MG1655 Δ*qseB* mutant, which we found to have impaired motility as previously reported (45). As expected, biofilm formation (Fig. 1A) was not altered when AI-2 was added to both motility mutants, nor did it affect MG1655 Δ*fliA* (reduction of motility was corroborated for this strain, too).

Deletion of *mqsR* decreases biofilm formation in 96-well plates and continuous flow system. Since *mqsR* is induced eightfold in biofilms (35) and is near *qseBC* (Fig. 3), we investigated its role in AI-2-controlled biofilm formation. Initially, we confirmed the impact of the *mqsR* deletion on biofilm formation of MG1655 by using 96-well plates after 24 h. Deletion of *mqsR* decreased biofilm formation in LB (74%), M9C glu (46%), and LB glu (78%) (Fig. 1B). Biofilm formation in flow cells corroborated these results (Table 3; Fig. 2C and D), since deleting *mqsR* at 48 h led to an 8-fold ± 14-fold reduction in biomass, a 19-fold ± 12-fold reduction in substratum coverage, and a 4-fold ± 3-fold change in thickness. Deleting *mqsR* changed the biofilm architecture significantly from a 54-μm-thick film with microcolonies to one with nearly no biomass (few colonies remaining). The 7.5-fold ± 4.6-fold increase in the roughness
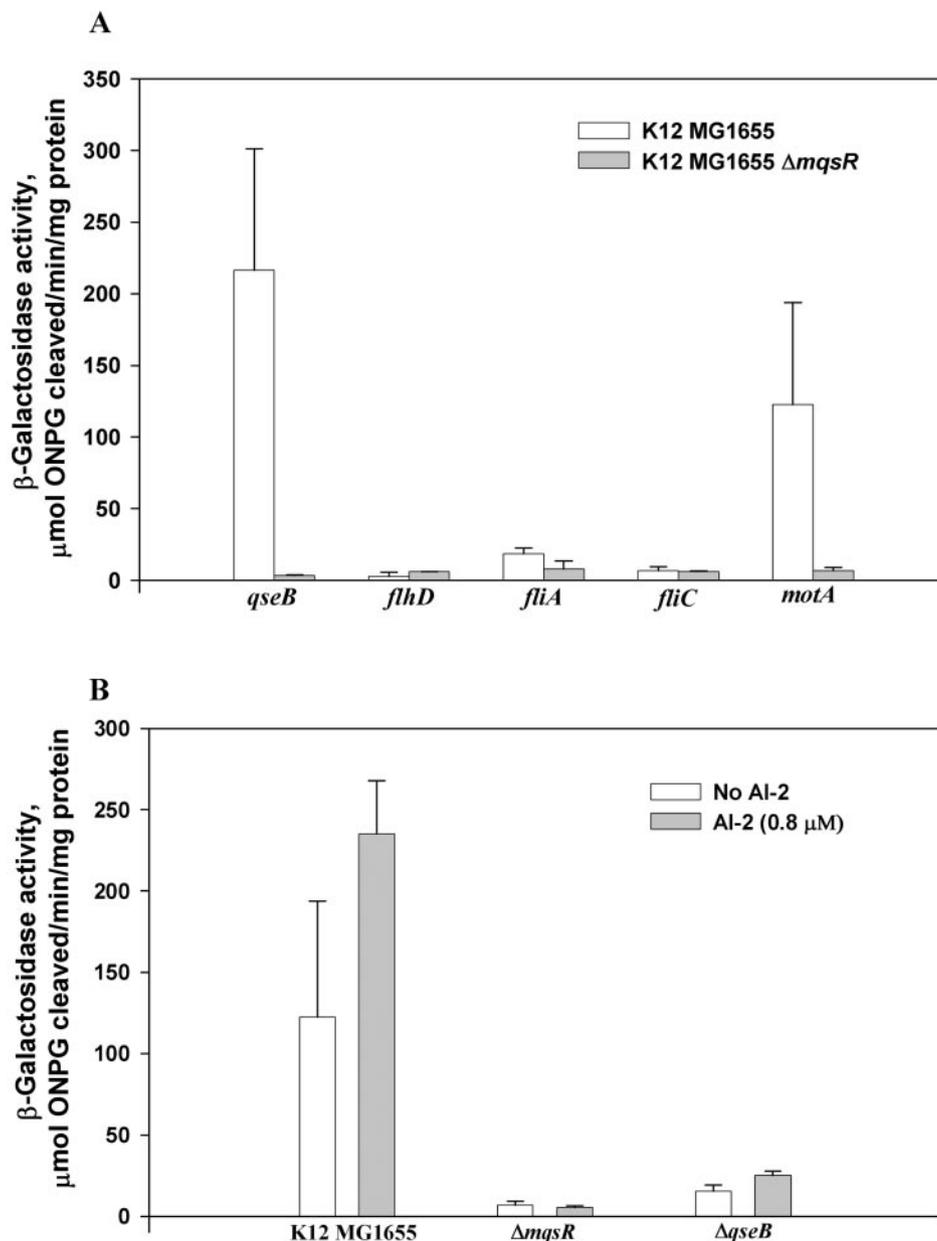
A

B

FIG. 5. (A) Effect of deleting *mqsR* on the transcription of *qseB*, *flhD*, *fliA*, *fliC*, and *motA* in MG1655 with M9C glu; (B) effect of adding AI-2 on the transcription of *motA* for the MG1655 deletion mutants Δ*mqsR* and Δ*qseB* in LB. The experiments were done in duplicate, and 1 standard deviation is shown.

coefficient (24 h) also indicated that there were few colonies formed after deletion of *mqsR*. Growth was not altered after *mqsR* was deleted, so the changes in the biofilm were not a result of growth rate differences; the specific growth rates in LB were 1.64 ± 0.02/h versus 1.720 ± 0.008/h for MG1655 and MG1655 Δ*mqsR*, respectively, while in M9C glu the specific growth rates were 0.990 ± 0.004/h versus 0.93 ± 0.03/h, respectively.

To corroborate that *mqsR* actually controls biofilm formation, we complemented *mqsR* in *trans* by constructing a low-copy-number plasmid (pVLT31) which expresses *mqsR*+ upon IPTG addition. By the addition of IPTG to MG1655Δ*mqsR*/

pVLT31 *mqsR*+ in LB medium, biofilm formation was restored from 30% of MG1655/pVLT31 at 0 mM IPTG to 84% at 0.2 mM IPTG; hence, MqsR regulates biofilm formation.

Note that the deletion of *fliA*, *qseB*, and *motA* also inhibited biofilm formation substantially (Fig. 1A and B). This appears to be the first report about the regulation of biofilm by QseB.

MqsR controls motility by regulating QseBC, FliA, and MotA. QseB and QseC are a two-component, quorum-sensing controlled regulator system for motility (45). We hypothesized that *mqsR* induces biofilm formation by regulating the two-component regulatory system *qseBC*, which then regulates the motility master regulon *flhD* (9). In agreement with this hy-

pothesis, we found that when *mqsR* was deleted, motility was abolished (Fig. 4). Furthermore, this lack of motility due to the deletion of *mqsR* was caused by a reduction in transcription of *qseB* (61-fold ± 27-fold), *fliA* (2.4-fold ± 2-fold), and *motA* (18-fold ± 10- fold) (Fig. 5A) in M9C glu. Similar results were found with LB, as *qseB*, *fliA*, and *motA* decreased 2.3-fold ± 1.4-fold, 5-fold ± 1-fold, and 11-fold ± 11-fold, respectively (results not shown). Note that although *flhD* transcription was not altered substantially in these experiments, its expression was altered greatly in the DNA microarrays (Table 4). To corroborate that *mqsR* abolishes motility, we complemented *mqsR* in *trans* with the low-copy-number plasmid pVLT31, which carries *mqsR*[+] (Fig. 4). Increasing the expression of *mqsR* by adding IPTG reestablished cell motility in a dose-dependent manner until it reached 50% of wild-type motility at 0.4 mM IPTG. Hence, MqsR regulates biofilm formation by inducing motility through QseBC.

MqsR is a global regulator in *E. coli* MG1655. Considering the size of MqsR (98 aa), we hypothesized it could be a global regulator in *E. coli*. To investigate this, differential gene expression was determined for MG1655 and MG1655 Δ*mqsR* in LB liquid culture. By deleting *mqsR*, 41 genes were downregulated >4-fold, while 33 genes were up-regulated >4-fold (Tables 4 and 5). Of the 246 genes that were down-regulated two- to ninefold, 14% (34 genes) were reported to be AI-2 controlled (15, 36, 44), which supplies additional evidence that MqsR is a global mediator between AI-2 and *E. coli*. Note that the genes that encode the master flagellum regulons *flhD* and *flhC* were down-regulated 24- and 7.5-fold, respectively, which also corroborates that MqsR regulates motility by controlling the master flagellum regulon *flhDC*. It was also found MqsR induced curli expression, based on its 26-fold differential expression of *crl* (Table 4), a transcriptional regulator of the cryptic *csgAB* locus for curli surface fibers (6), which has been reported to play a role in *E. coli* biofilm formation (7). The array results also showed that MqsR regulates motility by controlling not only QseB (Fig. 5A) but also *csrA*, which is downregulated in the *mqsR* mutant (twofold) and which regulates motility master regulon expression in *E. coli* (50).

MqsR links AI-2 quorum-sensing signal and biofilm formation. We tested the effect of the *mqsR* deletion on the ability of AI-2 to induce biofilm formation in LB by using microtiter plates. The addition of 6.4 μM AI-2 increased MG1655 biofilm mass by 2.8-fold ± 0.5-fold, while it had no effect when *mqsR* was deleted (Fig. 1A). Therefore, induction of biofilm formation by increasing motility is mediated by MqsR.

Induction of motility with AI-2 is mediated by MqsR and then QseBC. To corroborate the results obtained by Sperandio et al. (45), we measured the expression of *qseB* in MG1655 upon the addition of our synthesized AI-2 (0.8 μM). As expected, *qseB* transcription increased eightfold upon the addition of AI-2 (results not shown), while Sperandio et al. found sixfold induction by using preconditioned Dulbecco's modified Eagle medium. To find if the induction of motility with AI-2 was mediated by both MqsR and QseBC, we then measured *motA* expression in the *qseB* and *mqsR* mutants upon the addition of AI-2 (0.8 μM) and compared it to that of wild-type MG1655 (Fig. 5B). The addition of AI-2 induced *motA* activity for the wild-type strain but did not induce *motA* in the *mqsR*

TABLE 4. Repressed genes in suspension cultures due to the *mqsR* mutation (LB medium)[a]

Gene	b no.	Function	Expression ratio
yieI	b3716	Hypothetical protein	−27.9
crl	b0240	Transcriptional regulator of cryptic *csgA* gene for curli surface fibers	−26.0
flhD	**b1892**	**Regulator of flagellar biosynthesis, acting on class 2 operons**	**−24.3**
flu	b2000	CP4-44 prophage; phase-variable outer membrane-associated fluffing protein	−17.1
yncC	b1450	Hypothetical transcriptional regulator	−16.0
cynX	b0341	Cyanate transport	−14.9
ansP	b1453	L-Asparagine permease	−11.3
phnD	b4105	Periplasmic binding protein component of Pn transporter	−11.3
yeeR	b2001	CP4-44 prophage; putative membrane protein	−9.8
yeeL_2	b1979	AMP nucleosidase	−8.6
creD	b4400	Tolerance to colicin E2	−8.6
yjgL	b4253	Hypothetical protein	−8.0
flhC	**b1891**	**Regulator of flagellar biosynthesis acting on class 2 operons**	**−7.5**
yieJ	b3717	Hypothetical protein	−7.5
ydeV	b1511	Putative kinase	−7.0
ais	b2252	Protein induced by aluminum	−7.0
yraI	b3143	Putative chaperone	−7.0
ytfK	b4217	Hypothetical protein	−7.0
ycgW	b1160	Hypothetical protein	−6.5
yciE	b1257	Hypothetical protein	−6.5
yidS	**b3690**	**Hypothetical protein**	**−6.5**
ybbY	b0513	Possible uracil transporter	−5.7
yciF	b1258	Hypothetical protein	−5.7
yahO	**b0329**	**Hypothetical protein**	**−5.3**
yjcH	b4068	Hypothetical protein	−5.3
ydcV	b1443	Putative ABC transporter permease protein	−4.6
yncG	b1454	Hypothetical GST[b]-like protein	−4.6
spf	b3864	Nontranslated RNA	−4.6
yjcO	b4078	Hypothetical protein	−4.6
ymgB	**b1166**	**Hypothetical protein**	**−4.3**
ymgC	**b1167**	**Hypothetical protein**	**−4.3**
yeaQ	b1795	Hypothetical protein	−4.3
amyA	b1927	Cytoplasmic alpha-amylase	−4.3
gatC	**b2092**	**PTS[c] family enzyme IIC, galactitol specific**	**−4.3**
dsdX	b2365	Transport protein	−4.3
ygdI	b2809	Hypothetical protein	−4.3
b3254	**b3254**	**Hypothetical protein**	**−4.3**
yiaG	b3555	Hypothetical protein	−4.3
tra5_3	b0372	Putative transposase 5 of IS*3*	−4.0
yhjS	b3536	Hypothetical protein	−4.0
rbsC	b3750	D-Ribose high-affinity transport system	−4.0

[a] Genes consistently repressed ($P < 0.05$) more than fourfold are shown, and those in boldface type were reported regulated by AI-2 (15, 36, 44).
[b] GST, glutathione *S*-transferase.
[c] PTS, phosphotransferase.

and *qseB* mutants; therefore, the induction of motility was mediated by both MqsR and QseBC (Fig. 3).

Further evidence that *mqsR* is first in the cascade was provided by measuring the transcription of *qseB* with the wild-type strain and the *mqsR* mutant upon the addition of AI-2. If MqsR is first in the cascade and necessary for the transduction of the AI-2 signal, then the addition of AI-2 should only increase *qseB* transcription when *mqsR* is not deleted. We found that adding AI-2 at 6.4 μM induced the expression of *qseB* 3.2-fold in the wild-type strain in M9C glu but did not induce

TABLE 5. Induced genes in suspension cultures due to the *mqsR* mutation (LB medium)[a]

Gene	b no.	Function	Expression ratio
ymfI	b1143	Hypothetical protein	64.0
lit	b1139	Lit, cell death peptidase; phage exclusion; e14 prophage	52.0
pyrI	b4244	Aspartate carbamoyltransferase; PyrI subunit	36.8
pyrB	b4245	Aspartate carbamoyltransferase; PyrB subunit	34.3
yddK	b1471	Putative glycoportein	29.9
glpD	b3426	Glycerol 3-phosphate dehydrogenase; aerobic	26.0
ymfD	b1137	Hypothetical protein	24.3
glpK	b3926	Glycerol kinase	24.3
ymfK	**b1145**	**Putative phage repressor**	**21.1**
glpF	b3927	GlpF; glycerol MIP channel	14.9
aceB	b4014	Malate synthase	13.9
aceA	b4015	Isocitrate lyase monomer	13.9
glpA	b2241	Glycerol-3-phosphate-dehydrogenase, anaerobic	10.6
yiaM	b3577	YiaMNO binding protein-dependent secondary (TRAP)	10.6
ymfG	b1141	Hypothetical protein	9.8
ymfJ	b1144	Hypothetical protein	8.6
b1146	b1146	Hypothetical protein	8.6
ymfL	b1147	Hypothetical protein	8.6
ppdD	b0108	Prelipin peptidase-dependent protein	7.5
pyrL	b4246	*pyrBI* operon leader peptide	7.5
caiT	b0040	CaiT carnitine BCCT transporter	7.0
intE	b1140	Prophage e14 integrase	7.0
ykfG	b0247	Putative DNA repair protein	6.5
arp	b4017	Regulator of acetyl-CoA[b] synthetase	6.5
yzgL	b3427	Conserved protein	6.1
yncH	b1455	Hypothetical protein	5.3
mcrA	b1159	Restriction of DNA at 5-methylcytosine residues	4.9
yiaN	b3578	YiaMNO binding protein-dependent secondary (TRAP)	4.9
aceK	b4016	Isocitrate dehydrogenase phosphatase/isocitrate dehydrogenase kinase	4.6
yjgF	b4243	Conserved protein	4.6
oppB	b1244	Oligopeptide ABC transporter	4.3
oppD	b1246	Oligopeptide ABC transporter	4.0
asnU	b1986	tRNA	4.0

[a] Genes consistently induced ($P < 0.05$) more than fourfold are shown, and those in boldface type were reported regulated by AI-2 (15, 36, 44).
[b] CoA, coenzyme A.

FIG. 6. (A) Effect of adding AI-2 on the transcription of *qseB* in MG1655 and MG1655 Δ*mqsR* with M9C glu; (B) expression of *qseB* in MG1655 Δ*mqsR* with *mqsR* complemented in *trans* via IPTG induction. No effect of IPTG addition on expression of *qseB* was found with the negative control MG1655 Δ*mqsR*/pVLT31. The experiments were done in duplicate, and 1 standard deviation is shown.

qseB in the Δ*mqsR* mutant (Fig. 6A). As expected, the wild-type strain responded to AI-2 addition in a dose-dependent manner. To show further that MqsR is first in the cascade, the expression of *qseB* from pVS159 was also measured while inducing MqsR expression in *trans* in the Δ*mqsR* mutant by adding IPTG to strains harboring pVLT31 *mqsR*⁺. As expected if MqsR was required for signal transduction to QseB, expression of *qseB* was induced fourfold in a dose-dependent manner in M9C glu (Fig. 6B). Hence, MqsR is first in the cascade (Fig. 3).

DISCUSSION

We focused on *E. coli* biofilms, since this strain is the most thoroughly studied bacterium (5), its genome is sequenced
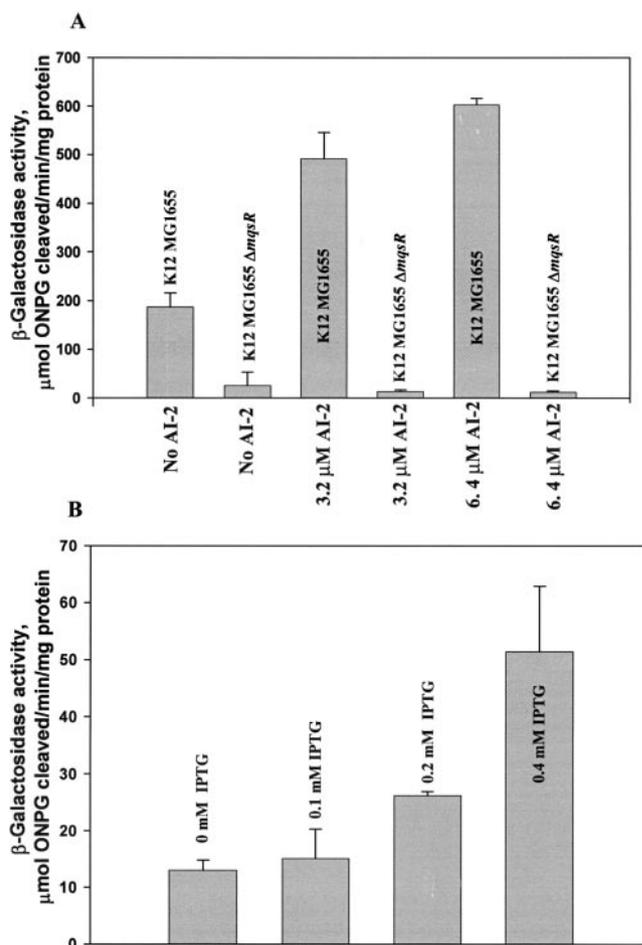
(5), microarrays are available (35, 42), the functions of many of its proteins have been elucidated (39), and many isogenic mutants are available (23). Also, our group has experience in determining the genetic basis of *E. coli* biofilm formation and its inhibition with natural, plant-derived antagonists (37, 38). Although *E. coli* is well studied, its biofilm has not received the same scrutiny, since many (but not all) K-12 strains make a poor biofilm if they lack a conjugative plasmid (18, 33).

In this study, we show that cross-species quorum-sensing signal AI-2 stimulates biofilm formation in five different *E. coli* hosts (ATCC 25404, MG1655, BW25113, DH5α, and JM109), in two different media (M9 citrate and LB), and in both batch and continuous flow systems (which enables the biofilm to be studied under two different hydrodynamic conditions, corroborates the results, and allows the biofilm architecture to be examined); hence, stimulation of biofilm formation by AI-2 is a general phenomenon. Our results here serve to explain two results that have been found previously: that AI-2 controls chemotaxis, flagellar synthesis, and motility in *E. coli* (36, 44)

and that the quorum-sensing antagonist furanone was effective in preventing the biofilms of *E. coli* by repressing these same chemotaxis, flagellar synthesis, and motility genes (36). Therefore, AI-2 stimulates biofilm formation directly, flagellar synthesis and motility are clearly involved in biofilm formation, and furanone inhibits biofilm formation by masking AI-2.

We have also shown here that AI-2 stimulates biofilm formation by increasing motility, since addition of AI-2 stimulated the motility of two strains (ATCC 25404 and MG1655), since AI-2 addition had no effect on the biofilm formation of the motility-impaired mutants *motA* and *qseB* (Fig. 1A), since the transcription of flagellar genes is induced by AI-2, and since the biomass, substratum coverage, and biofilm thickness of the *luxS* mutant *E. coli* DH5α, which has abolished motility, are less than those of *E. coli* ATCC 25404 with AI-2 (Table 3). Furthermore, by stimulating motility, the addition of AI-2 changes the architecture of the ATCC 25404 biofilm to a flatter phenotype in flow cells (Fig. 2). Previous reports have indicated that motility plays an important role in the attachment of cells to the surface (32), but here we show that motility (stimulated by AI-2) affects the architecture, too.

Previous reports have indicated AI-2 is not necessary for mature biofilm formation when a conjugation plasmid such as R1*drd*19 is present in minimal AB medium with glucose (33). Here, along with one of the first applications of synthesized AI-2, we used wild-type strains that lack a conjugation plasmid and were cultured in rich medium and found AI-2 plays a surprisingly large role in biofilm formation (25-fold). The difference in results was most likely due to the lack of the conjugation plasmid, as we showed here (Fig. 1A), as well as to the difference in hosts used (that is one reason we verified our results with five familiar strains). Contrary to previous reports (18), the wild-type strain (MG1655) harboring the conjugative plasmid forms less biofilm in the presence of AI-2 than the non-plasmid-carrying strain (Fig. 1A). One explanation may be that we found that the addition of conjugation plasmids induces biofilm formation by inducing cell aggregation, not by changing motility (18a). We believe that cells harboring R1*drd*19 in the presence of AI-2 have induced motility, which may impede cell aggregation and thereby decrease biofilm formation. The fact that we saw the smallest stimulation of both biofilm formation and motility with AI-2 for JM109 corroborates this, since JM109 contains the F′ conjugation plasmid.

We also found that AI-2 stimulates biofilm formation via the uncharacterized protein MqsR by showing that MqsR induces motility (Fig. 4) and biofilm formation in both batch and continuous systems (Fig. 1B and 2), that AI-2 stimulates motility through MotA (Fig. 5B) and biofilm formation through MqsR (Fig. 1A), and that MqsR stimulates QseB (Fig. 5A), which controls motility in *E. coli*. Previous reports have found relationships between quorum sensing and biofilms (28), but these reports have not found the genetic underpinnings behind the biofilm phenotype. Based on the discovery in the present work that AI-2 stimulates biofilms directly, we propose a genetic model (Fig. 3) for how AI-2 controls biofilm formation in *E. coli*. Sperandio et al. (45) found the link between AI-2 and motility for the two-component regulatory system *qseBC*, yet they proposed that additional regulators in the cascade that mediate motility and quorum sensing need to be found and characterized. One of these links is now found, and it connects AI-2, MqsR, QseBC, and biofilm formation.

Our model (Fig. 3) is that AI-2 stimulates biofilm formation by stimulating expression of MqsR, which then directly or indirectly induces expression of QseBC, which then promotes cell motility via the master regulon *flhDC*, which then stimulates MotA and FliA and leads to biofilm formation. Without this stimulation of motility, biofilm formation is severely impaired (Fig. 1). We found that *qseB* is controlled by MqsR (Fig. 5A) and that MqsR controls *flhDC* (Table 4) and therefore motility. We also found that MqsR induces curli expression through *crl* (Table 4) and possibly induces motility through *csrA*. Hence, MqsR controls biofilm formation by inducing motility and curli synthesis. Considering that MqsR controls 108 proteins with unknown functions (Tables 4 and 5) and that MqsR is a global AI-2-controlled regulator, there are many new proteins to investigate in regard to biofilm formation, control, and quorum sensing.

In summary, we have determined that the species-nonspecific, quorum signal AI-2 directly stimulates biofilm formation in *E. coli*, that the mechanism is through stimulating motility genes, and that MqsR mediates this effect prior to QseBC. These results serve to make sense of our previous microarray data and serve to give a deeper understanding of how plant biofilm inhibitors work. Hence, our results are helpful for understanding and preventing biofilm formation by the archetypal strain, as well as helpful for combating related pathogenic strains such as *E. coli* O157:H7 (30).

REFERENCES

1. **Baba, T., T. Ara, Y. Okumura, M. I. Hasegawa, Y. Takai, M. Baba, T. Oshima, et al.** Systematic construction of single gene deletion mutants in *Escherichia coli* K-12. Unpublished data.
2. **Balestrino, D., J. A. J. Haagensen, C. Rich, and C. Forestier.** 2005. Characterization of type 2 quorum sensing in *Klebsiella pneumoniae* and relationship with biofilm formation. J. Bacteriol. **187:**2870–2880.
3. **Bassler, B. L.** 1999. How bacteria talk to each other: regulation of gene expression by quorum sensing. Curr. Opin. Microbiol. **2:**582–587.
4. **Bassler, B. L., E. P. Greenberg, and A. M. Stevens.** 1997. Cross-species induction of luminescence in the quorum-sensing bacterium *Vibrio harveyi*. J. Bacteriol. **179:**4043–4045.
5. **Blattner, F. R., G. Plunkett III, C. A. Bloch, N. T. Perna, V. Burland, M. Riley, J. Collado-Vides, J. D. Glasner, C. K. Rode, G. F. Mayhew, J. Gregor, N. W. Davis, H. A. Kirkpatrick, M. A. Goeden, D. J. Rose, B. Mau, and Y. Shao.** 1997. The complete genome sequence of *Escherichia coli* K-12. Science **277:**1453–1474.
6. **Bougdour, A., C. Lelong, and J. Geiselmann.** 2004. Crl, a low temperature-induced protein in *Escherichia coli* that binds directly to the stationary phase σ subunit of RNA polymerase. J. Biol. Chem. **279:**19540–19550.
7. **Brombacher, E., C. Dorel, A. J. B. Zehnder, and P. Landini.** 2003. The curli biosynthesis regulator CsgD co-ordinates the expression of both positive and negative determinants for biofilm formation in *Escherichia coli*. Microbiology **149:**2847–2857.
8. **Chain, P. S. G., E. Carniel, F. W. Larimer, J. Lamerdin, P. O. Stoutland, W. M. Regala, A. M. Georgescu, et al.** 2004. Insights into the evolution of *Yersinia pestis* through whole-genome comparison with *Yersinia pseudotuberculosis*. Proc. Natl. Acad. Sci. USA **101:**13826–13831.
9. **Chilcott, G. S., and K. T. Hughes.** 2000. Coupling of flagellar gene expression to flagellar assembly in *Salmonella enterica* serovar Typhimurium and *Escherichia coli*. Microbiol. Mol. Biol. Rev. **64:**694–708.

10. **Cole, S. P., J. Hardwood, R. Lee, R. She, and D. G. Guiney.** 2004. Characterization of monospecies biofilm formation by *Helicobacter pylori*. J. Bacteriol. **186:**3124–3132.

11. **Costerton, J. W., P. S. Stewart, and E. P. Greenberg.** 1999. Bacterial biofilms: a common cause of persistent infections. Science **284:**1318–1322.

12. **Daines, D. A., M. Bothwell, J. Furrer, K. Unrath, K. Nelson, J. Jarisch, N. Melrose, L. Greiner, M. Apicella, and A. L. Smith.** 2005. *Haemophilus influenzae luxS* mutants form a biofilm and have increased virulence. Microb. Pathog. **39:**87–96.

13. **Datsenko, K. A., and B. L. Wanner.** 2000. One-step inactivation of chromosomal genes in *Escherichia coli* K-12 using PCR products. Proc. Natl. Acad. Sci. USA **97:**6640–6645.

14. **Davies, D. G., M. R. Parsek, J. P. Pearson, B. H. Iglewski, J. W. Costerton, and E. P. Greenberg.** 1998. The involvement of cell-to-cell signals in the development of a bacterial biofilm. Science **280:**295–298.

15. **DeLisa, M. P., C.-F. Wu, L. Wang, J. J. Valdes, and W. E. Bentley.** 2001. DNA microarray-based identification of genes controlled by autoinducer 2-stimulated quorum sensing in *Escherichia coli*. J. Bacteriol. **183:**5239–5247.

16. **de Lorenzo, V., L. Eltis, B. Kessler, and K. N. Timmis.** 1993. Analysis of *Pseudomonas* gene products using *lacI*q/*Ptrp-lac* plasmids and transposons that confer conditional phenotypes. Gene **123:**17–24.

17. **Fishman, A., Y. Tao, L. Rui, and T. K. Wood.** 2005. Controlling the regiospecific oxidation of aromatics via active site engineering of toluene *para*-monooxygenase of *Ralstonia pickettii* PKO1. J. Biol. Chem. **280:**506–514.

18. **Ghigo, J.-M.** 2001. Natural conjugative plasmids induce bacterial biofilm development. Nature **412:**442–445.

18a. **A. F. González Barrios, R. Zuo, D. Ren, and T. K. Wood.** Hha, YbaJ, and OmpA regulate *Escherichia coli* K12 biofilm formation and conjugation plasmids abolish motility. Biotechnol. Bioeng., in press.

19. **Hammer, B. K., and B. L. Bassler.** 2003. Quorum sensing controls biofilm formation in *Vibrio cholerae*. Mol. Microbiol. **50:**101–114.

20. **Hansen, M. C., R. J. Palmer, Jr., C. Udsen, D. C. White, and S. Molin.** 2001. Assessment of GFP fluorescence in cells of *Streptococcus gordonii* under conditions of low pH and low oxygen concentration. Microbiology **147:**1383–1391.

21. **Hashimoto, Y., L. Wang, C.-Y. Tsao, L. Yang, Y. Um, T. K. Wood, J. J. Valdes, and W. E. Bentley.** On the in vitro reaction of *S*-adenosylhomocysteine with AI-2 synthases, Pfs and LuxS: alternative pathways to AI-2 like autoinducers. Submitted for publication.

22. **Heydorn, A., A. T. Nielsen, M. Hentzer, C. Sternberg, M. Givskov, B. K. Ersbøll, and S. Molin.** 2000. Quantification of biofilm structures by the novel computer program COMSTAT. Microbiology **146:**2395–2407.

23. **Kang, Y., T. Durfee, J. D. Glasner, Y. Qiu, D. Frisch, K. M. Wintemberg, and F. R. Blattner.** 2004. Systematic mutagenesis of the *Escherichia coli* genome. J. Bacteriol. **186:**4921–4930.

24. **Labbate, M., S. Y. Queck, K. S. Koh, S. A. Rice, M. Givskov, and S. Kjelleberg.** 2004. Quorum-sensing-controlled biofilm development in *Serratia liquefaciens* MG1. J. Bacteriol. **186:**692–698.

25. **Li, Y.-H., P. C. Y. Lau, J. H. Lee, R. P. Ellen, and D. G. Cvitkovitch.** 2001. Natural genetic transformation of *Streptococcus mutans* growing in biofilms. J. Bacteriol. **183:**897–908.

26. **McNab, R., S. K. Ford, A. El-Sabaeny, B. Barbieri, G. S. Cook, and R. Lamont.** 2003. LuxS-based signaling in *Streptococcus gordonii*: autoinducer 2 controls carbohydrate metabolism and biofilm formation with *Porphyromonas gingivalis*. J. Bacteriol. **185:**274–284.

27. **Parkhill, J., M. Sebaihia, A. Preston, L. D. Murphy, N. Thomson, D. E. Harris, M. T. Holden, et al.** 2003. Comparative analysis of the genome sequences of *Bordetella pertussis*, *Bordetella parapertussis* and *Bordetella bronchiseptica*. Nat. Genet. **35:**32–40.

28. **Parsek, M. R., and E. P. Greenberg.** 2005. Sociomicrobiology: the connections between quorum sensing and biofilms. Trends Microbiol. **13:**27–33.

29. **Paulsen, I. T., C. M. Press, J. Ravel, D. Y. Kobayashi, G. S. A. Myers, D. V. Mavrodi, R. T. DeBoy, et al.** 2005. Complete genome sequence of the plant commensal *Pseudomonas fluorescens* Pf-5. Nat. Biotechnol. **23:**873–878.

30. **Perna, N. T., G. Plunkett III, V. Burland, B. Mau, J. D. Glasner, D. J. Rose, G. F. Mayhew, et al.** 2001. Genome sequence of enterohaemorrhagic *Escherichia coli* O157:H7. Nature **409:**529–533.

31. **Potera, C.** 1999. Forging a link between biofilms and disease. Science **283:**1837–1839.

32. **Pratt, L. A., and R. Kolter.** 1998. Genetic analysis of *Escherichia coli* biofilm formation: roles of flagella, motility, chemotaxis and type I pili. Mol. Microbiol. **30:**285–293.

33. **Reisner, A., J. A. J. Haagensen, M. A. Schembri, E. L. Zechner, and S. Molin.** 2003. Development and maturation of *Escherichia coli* K-12 biofilms. Mol. Microbiol. **48:**933–946.

34. **Ren, D., L. Bedzyk, P. Setlow, S. Thomas, R. W. Ye, and T. K. Wood.** 2004. Gene expression in *Bacillus subtilis* surface biofilms with and without sporulation and the importance of *yveR* for biofilm maintenance. Biotechnol. Bioeng. **86:**344–364.

35. **Ren, D., L. Bedzyk, S. Thomas, R. W. Ye, and T. K. Wood.** 2004. Gene expression in *Escherichia coli* biofilms. Appl. Microbiol. Biotechnol. **64:**515–524.

36. **Ren, D., L. Bedzyk, R. W. Ye, S. Thomas, and T. K. Wood.** 2004. Differential gene expression shows natural brominated furanones interfere with the autoinducer-2 bacterial signaling system of *Escherichia coli*. Biotechnol. Bioeng. **88:**630–642.

37. **Ren, D., J. J. Sims, and T. K. Wood.** 2001. Inhibition of biofilm formation and swarming of *Escherichia coli* by (5Z)-4-bromo-5-(bromomethylene)-3-butyl-2(5H)-furanone. Environ. Microbiol. **3:**731–736.

38. **Ren, D., R. Zuo, A. F. González Barrios, L. A. Bedzyk, G. R. Eldridge, M. E. Pasmore, and T. K. Wood.** 2005. Differential gene expression for investigation of *Escherichia coli* biofilm inhibition by plant extract ursolic acid. Appl. Environ. Microbiol. **71:**4022–4034.

39. **Riley, M., and B. Labedan (ed.).** 1996. *Escherichia coli* genes products: physiological functions and common ancestries, 2nd ed. ASM Press, Washington, D.C.

40. **Rodriguez, R. L., and R. C. Tait.** 1983. Recombinant DNA techniques: an introduction. Benjamin/Cummings Publishing, Menlo Park, Calif.

41. **Sambrook, J., E. F. Fritsch, and T. Maniatis.** 1989. Molecular cloning: a laboratory manual, 2nd ed. Cold Spring Harbor Laboratory Press, Cold Spring Harbor, N.Y.

42. **Selinger, D. W., K. J. Cheung, R. Mei, E. M. Johansson, C. S. Richmond, F. R. Blattner, D. J. Lockhart, et al.** 2000. RNA expression analysis using a 30 base pair resolution *Escherichia coli* genome array. Nat. Biotechnol. **18:**1262–1268.

43. **Song, Y., Z. Tong, J. Wang, L. Wang, Z. Guo, Y. Han, J. Zhang, et al.** 2004. Complete genome sequence of *Yersinia pestis* strain 91001, an isolate avirulent to humans. DNA Res. **11:**179–197.

44. **Sperandio, V., A. G. Torres, J. A. Giron, and J. B. Kaper.** 2001. Quorum sensing is a global regulatory mechanism in enterohemorrhagic *Escherichia coli* O157:H7. J. Bacteriol. **183:**5187–5197.

45. **Sperandio, V., A. G. Torres, and J. B. Kaper.** 2002. Quorum sensing *Escherichia coli* regulators B and C (QseBC): a novel two-component regulatory system involved in the regulation of flagella and motility by quorum sensing in *E. coli*. Mol. Microbiol. **43:**809–821.

46. **Surette, M. G., and B. L. Bassler.** 1998. Quorum sensing in *Escherichia coli* and *Salmonella typhimurium*. Proc. Natl. Acad. Sci. USA **95:**7046–7050.

47. **Surette, M. G., M. B. Miller, and B. L. Bassler.** 1999. Quorum sensing in *Escherichia coli*, *Salmonella typhimurium*, and *Vibrio harveyi*: a new family of genes responsible for autoinducer production. Proc. Natl. Acad. Sci. USA **96:**1639–1644.

48. **Toussaint, A., C. Merlin, S. Monchy, M. A. Benotmane, R. Leplae, M. Mergeay, and D. Springael.** 2003. The biphenyl- and 4-chlorobiphenyl-catabolic transposon Tn*4371*, a member of a new family of genomic islands related to IncP and Ti plasmids. Appl. Environ. Microbiol. **69:**4837–4845.

49. **Wang, L., Y. Hashimoto, C.-Y. Tsao, J. J. Valdes, and W. E. Bentley.** 2005. Cyclic AMP (cAMP) and cAMP receptor protein influence both synthesis and uptake of extracellular autoinducer 2 in *Escherichia coli*. J. Bacteriol. **187:**2066–2076.

50. **Wei, B. L., A.-M. Brun-Zinkernagel, J. W. Simecka, B. M. Prüß, P. Babitzke, and T. Romeo.** 2001. Positive regulation of motility and *flhDC* expression by the RNA-binding protein CsrA of *Escherichia coli*. Mol. Microbiol. **40:**245–256.

51. **Wood, T. K., and S. W. Peretti.** 1991. Effect of chemically-induced, cloned-gene expression on protein synthesis in *E. coli*. Biotechnol. Bioeng. **38:**397–412.

52. **Xavier, K. B., and B. L. Bassler.** 2003. LuxS quorum sensing: more than just a numbers game. Curr. Opin. Microbiol. **6:**191–197.

53. **Xavier, K. B., and B. L. Bassler.** 2005. Regulation of uptake and processing of the quorum-sensing autoinducer AI-2 in *Escherichia coli*. J. Bacteriol. **187:**238–248.

54. **Yanisch-Perron, C., J. Viera, and J. Messing.** 1985. Improved M13 phage cloning vectors and host strains: nucleotide sequences of the M13mp18 and pUC19 vectors. Gene **33:**103–119.